EUKARYOTIC CELL, Feb. 2005, p. 281–288 Vol. 4, No. 2
1535-9778/05/$08.00+0 doi:10.1128/EC.4.2.281–288.2005

Interaction among Btn1p, Btn2p, and Ist2p Reveals Potential Interplay among the Vacuole, Amino Acid Levels, and Ion Homeostasis in the Yeast *Saccharomyces cerevisiae*

Yoojin Kim,[1]† Subrata Chattopadhyay,[1] Sarahjane Locke,[1] and David A. Pearce[1,2,3]*

Center for Aging and Developmental Biology, Aab Institute of Biomedical Sciences,[1] Department of Biochemistry and Biophysics,[2] and Department of Neurology,[3] School of Medicine and Dentistry, University of Rochester, Rochester, New York

Received 12 August 2004/Accepted 11 November 2004

Btn2p, a novel cytosolic coiled-coil protein in *Saccharomyces cerevisiae*, was previously shown to interact with and to be necessary for the correct localization of Rhb1p, a regulator of arginine uptake, and Yif1p, a Golgi protein. We now report the biochemical and physical interactions of Btn2p with Ist2p, a plasma membrane protein that is thought to have a function in salt tolerance. A deletion in Btn2p (*btn2*Δ strains) results in a failure to correctly localize Ist2p, and strains lacking Btn2p and Ist2p (*btn2*Δ *ist2*Δ strains) are unable to grow in the presence of 0.5 or 1.0 M NaCl. Btn2p was originally identified as being up-regulated in a *btn1*Δ strain, which lacks the vacuolar-lysosomal membrane protein, Btn1p, and serves as a model for Batten disease. This up-regulation of Btn2p was shown to contribute to the maintenance of a stable vacuolar pH in the *btn1*Δ strain. Btn1p was subsequently shown to be required for the optimal transport of arginine into the vacuole. Interestingly, *btn1*Δ *ist2*Δ strains are also unable to grow in the presence of 0.5 or 1.0 M NaCl, and *ist2*Δ suppresses the vacuolar arginine transport defect in *btn1*Δ strains. Although further investigation is required, we speculate that altered vacuolar arginine transport in *btn1*Δ strains represents a mechanism for maintaining or balancing cellular ion homeostasis. Btn2p interacts with at least three proteins that are seemingly involved in different biological functions in different subcellular locations. Due to these multiple interactions, we conclude that Btn2p may play a regulatory role across the cell in response to alterations in the intracellular environment that may be caused by changes in amino acid levels or pH, a disruption in protein trafficking, or imbalances in ion homeostasis resulting from either genetic or environmental manipulation.

BTN2 in the yeast *Saccharomyces cerevisiae* encodes a nonessential novel coiled-coil protein, Btn2p, which was originally identified by gene expression profiling as one of only two proteins up-regulated in yeast strains lacking Btn1p (*btn1*Δ strains), the yeast model for Batten disease (24). This up-regulation of Btn2p in *btn1*Δ strains was originally presumed to occur in response to altered vacuolar pH because deletion of either *BTN1* or *BTN2* results in an alteration of the ability of yeast cells to maintain balanced pH homeostasis in the vacuole (1, 24). It was subsequently determined that Btn2p interacts with Rhb1p (previously designated Rsg1p), which regulates the activity of plasma membrane Can1p arginine and lysine permease (2, 27). Furthermore, deletion of *BTN2* results in altered arginine uptake, a phenotype exhibited by *rhb1*Δ strains. This altered arginine uptake in *btn2*Δ strains was shown to result from a failure to localize Rhb1p to a distinct peripheral structure, thereby causing a loss of the regulation of arginine uptake by the Can1p permease (2). Therefore, Btn2p was implicated in regulating intracellular levels of arginine, an assertion supported by the fact that Btn1p has been shown to have a role in the transport of arginine across the vacuolar membrane (12). Thus, the original observation that Btn2p was up-regulated in *btn1*Δ strains was interpreted to be a compensatory mechanism for balancing intracellular arginine levels, although the functions of both Btn1p and Btn2p still require further study.

Btn2p has also been shown to interact with Yif1p (3), an essential protein that is a component of a complex at the Golgi apparatus that interacts with transport GTPases, such as Ypt1p, Ypt31p, and Sec4p, and that functions in transport from the endoplasmic reticulum to the Golgi apparatus (16). In the absence of Btn2p (*btn2*Δ strains), Yif1p becomes mislocalized to or accumulates in the vacuole. Therefore, disruption of Btn2p function alters the trafficking of both Rhb1p and Yif1p, which have different functions in different parts of the cell. These results implicate Btn2p as having a function in intracellular protein trafficking and in maintaining intracellular metabolite homeostasis and suggest that disturbances in intracellular homeostasis and protein trafficking may be linked.

We report a third protein interaction for Btn2p. We demonstrate that Ist2p, a plasma membrane protein that has been reported to show homology to sodium and calcium channel proteins (15) and to have a function in salt tolerance (5), interacts physically and biochemically with Btn2p. Similar to the situation for other Btn2p-interacting proteins, the disruption of Btn2p function results in a failure to correctly localize Ist2p. Moreover, the disruption of both Btn2p and Ist2p (*btn2*Δ *ist2*Δ strains) reveals a potential functional interaction between these two proteins through sensitivity of growth in the presence of NaCl. Therefore, *btn2*Δ results in the altered subcellular

* Corresponding author. Mailing address: Center for Aging and Developmental Biology, Box 645, School of Medicine and Dentistry, University of Rochester, Rochester, NY 14642. Phone: (585) 273-1514. Fax: (585) 506-1972. E-mail: david_pearce@urmc.rochester.edu.

† Present address: Vollum Institute, Oregon Health Sciences University, Portland, OR 97239.

TABLE 1. Yeast strains used in this study

Genotype	Strain
MATα his3Δ1 leu2Δ0 lys2Δ0 ura3Δ0	B-11718
MATα btn1Δ::KanMX his3Δ1 leu2Δ0 lys2Δ0 ura3Δ0	B-13048
MATα btn2Δ::KanMX his3Δ1 leu2Δ0 lys2Δ0 ura3Δ0	B-14847
MATα rhb1Δ::KanMX his3Δ1 leu2Δ0 lys2Δ0 ura3Δ0	B-14248
MATα ist2Δ::KanMX his3Δ1 leu2Δ0 lys2Δ0 ura3Δ0	B-14884
MATα btn2Δ::loxP rhb1Δ::KanMX his3Δ1 leu2Δ0 lys2Δ0 ura3Δ0	B-14399
MATα btn1Δ::loxP rhb1Δ::KanMX his3Δ1 leu2Δ0 lys2Δ0 ura3Δ0	B-14252
MATα btn2Δ::loxP ist2Δ::KanMX his3Δ1 leu2Δ0 lys2Δ0 ura3Δ0	B-15013
MATα btn1Δ::loxP ist2Δ::KanMX his3Δ1 leu2Δ0 lys2Δ0 ura3Δ0	B-14830
MATα btn1Δ::loxP btn2Δ::KanMX his3Δ1 leu2Δ0 lys2Δ0 ura3Δ0	B-13049
MATα leu2-3,112 ura3-52 his3-200 ade2-101 lys2-801 trp1-901 cdc25-2	CDC25H
*MAT***a** *leu2Δ1 ura3-52 his3-200 ade2-101 lys2-801 trp1Δ63*	YPH499
MATα ist2Δ::KanMX his3Δ1 leu2Δ0 lys2Δ0 ura3Δ0 + pDAP124	B-14915
MATα btn2Δ::loxP ist2Δ::KanMX his3Δ1 leu2Δ0 lys2Δ0 ura3Δ0 + pDAP0124	B-14983

localization of the interacting proteins Rhb1p, Yif1p, and Ist2p, which have been implicated in a variety of cellular processes, such that *btn2*Δ results in pleiotrophic phenotypes. Therefore, the up-regulation of Btn2p in *btn1*Δ strains may represent a compensatory mechanism for balancing disturbances in each of these biological processes, namely, the regulation of amino acid levels, protein trafficking, and ion homeostasis. In addition, we demonstrate that *btn1*Δ *ist2*Δ strains also exhibit NaCl sensitivity and that *ist2*Δ can suppress the vacuolar arginine transport defect in *btn1*Δ strains. As human Cln3 has been shown to complement Btn1p function in *btn1*Δ strains (9, 12, 23), the implications of these results are also discussed in the context of Batten disease.

MATERIALS AND METHODS

Yeast strains and plasmids. The *S. cerevisiae* strains used in this work are listed in Table 1. Strain B-11718 was acquired from the American Type Culture Collection, and strain YPH499 was obtained from Stratagene. Strains B-13048 (*btn1*Δ), B-14248 (*rhb1*Δ), B-14252 (*btn1*Δ *rhb1*Δ), and B-14399 (*btn2*Δ *rhb1*Δ) were previously described (2).

Strains constructed for this study were generated by using the *loxP-KanMX-loxP* disruption cassette (7). The *btn2*::*loxP-KanMX-loxP* disruption cassette was amplified by using forward primer 5′-CAA CCA AAA GAA AAT AAC TAA TAG ACC CCA TTA CAA TAT AGA AGC ATA GGC CAC TAG TGG ATC TG-3′ and reverse primer 5′-GCC GTA AAA ATG AAA GAT GGG GAG TAT GTA TTA TCA CCC ACA GCT GAA GCT TCG AC GC-3′. The *ist2*::*loxP-KanMX-loxP* disruption cassette was amplified by using forward primer 5′-ATG TCG CAG ACA ATT ACA TCT CTA GAT CCG AAT TGT GTT AGC ATA GGC CAC TAG TGG ATC TG-3′ and reverse primer 5′-AGA GGA TTC GGT TGT CTT AGA ATT GTT CGT GAC ATT CTT CAC TCC AGC TGA AGC TTC GTA CGC-3′. The *btn1*::*loxP-KanMX-loxP* disruption cassette was amplified by using forward primer 5′-GTA CTT AAA CAC ATA TGA AGA TAT AGC GCA AGT AAA TAT AAG CAT AGG CCA CTA GTG GAT CTG-3′ and reverse primer 5′-CAC TTT ATT TCA ATC TCC TAT TTA ATA TCA CAA CAA AAC TCA GCT GAA GCT TCG TAC GC-3′. Plasmid pCP132 served as the template to generate all *loxP-KanMX-loxP* disruption cassettes.

Strains B-14847 (*btn2*Δ) and B-14884 (*ist2*Δ) were constructed by transforming B-11718 competent cells with PCR-generated *btn2*::*loxP-KanMX-loxP* and *ist2*::*loxP-KanMX-loxP* gene disruption cassettes, respectively. Strain B-14830 (*btn1*Δ *ist2*Δ) was generated by transforming B-14884 (*ist2*Δ) competent cells with the PCR-generated *btn1*::*loxP-KanMX-loxP* gene disruption cassette. Strain B-15013 (*btn2*Δ *ist2*Δ) was constructed by transforming B-14847 with *ist2*::*loxP-KanMX-loxP* followed by excision of the *KanMX* selection marker by using the Cre-*loxP* recombination event. The transformants were selected on YPD medium (2% glucose, 1% Bacto yeast extract, 2% Bacto peptone) supplemented with 200 μg of Geneticin (G-418 sulfate; Invitrogen)/ml.

All integration events were verified by PCR analyses. The primers used in the PCR to validate replacement of the genes were kanFW (5′-CCT CGA CAT CAT CTG CCC-3′) and kanRE (5′-GGA TGT ATG GGC TAA ATG-3′). These primers anneal to regions inside the two *loxP* sequences. Also, primers annealing to regions 350 to 500 bp upstream of the ATG translational start site and 350 to 500 bp downstream of the stop codon of *BTN1*, *BTN2*, or *IST2* were used in combination with primers kanFW and kanRE to confirm homologous integration at the desired locus.

Double-deletion strains were constructed by using the Cre-*loxP* recombination technique. Plasmid pCP133 contains the Cre recombinase gene under the control of the *GAL1* promoter. Expression of the Cre recombinase results in precise excision of the *KanMX* marker, allowing for the selection marker to be reused for the construction of double-deletion strains. The primers used to validate homologous integration (see above) were used to confirm excision of the *KanMX* marker at the *BTN2* or *IST2* locus. Plasmid pCP133 was removed from each of the strains lacking the *KanMX* marker by streaking 10^6 cells onto a solid medium (2% glucose and 0.67% yeast nitrogen base with amino acids) containing 5-fluoroorotic acid and selecting for uracil auxotrophs.

For complementation studies, *IST2*–c-*myc* and enhanced green fluorescent protein (EGFP)-*IST2* were independently subcloned into centromeric single-copy expression vector pAB625 (1).

NaCl sensitivity. To assay NaCl sensitivity, growth on agar-solidified media was assessed by spotting 5 μl of cell suspension containing approximately 10^5, 10^4, 10^3, 10^2, or 10^1 cells onto YPD medium, YPD medium–0.5 M NaCl, or YPD medium–1.0 M NaCl. The plates were incubated for 2 to 3 days at 30°C.

Two-hybrid studies and coimmunoprecipitation of Btn2p and Ist2p. The Stratagene Cytotrap system was used for two-hybrid screening of interaction partners for Btn2p. The manufacturer's instructions were essentially followed with *BTN2*-pSOS, a bait plasmid screened as previously described against a yeast cDNA library constructed in the pMyr or trap plasmid (2).

BTN2 and *IST2* were cloned into yeast epitope tagging vector pESC-TRP (Stratagene). Plasmid DAP114 contains the *BTN2* open reading frame (ORF) tagged with the FLAG epitope at the 3′ terminus and the *IST2* ORF tagged with the c-*myc* epitope at the 3′ terminus. *BTN2* was cloned as previously described (2). For *IST2*, an ApaI restriction site was introduced at the 5′ end and a SalI site was introduced at the 3′ end of a PCR-amplified fragment of *IST2* by using primers with the sequences 5′-GGG CCC ATG TCG CAG ACA ATT AC-3′ and 5′-GTC GAC AAG CTT CTT TTT CAG CTT ATG-3′. Amplified *IST2* was cloned into pCR-Blunt (Invitrogen), resulting in DAP106.

The plasmid containing *BTN2*-FLAG and *IST2*–c-*myc* was transformed into yeast strain YPH499 (Table 1). Protein-protein interactions were confirmed by immunoprecipitation followed by Western analysis as previously described (2). The blot was probed with anti-c-*myc* mouse monoclonal antibody (1:1,000; Neomarkers) or anti-FLAG mouse monoclonal antibody (Sigma) and with horseradish peroxidase-tagged anti-mouse secondary antibody (1:3,000; Amersham). The blot was stained by using an ECLplus kit (Amersham) and developed on ECL film.

Localization of EGFP-Btn2p and EGFP-Ist2p. EGFP-Btn2p was previously described (2). Plasmid DAP124 contains yeast EGFP at the N terminus of the *IST2* ORF, which is downstream of the *MET* promoter. To construct plasmid DAP124, a 2,885-bp BamHI/SalI fragment containing the *IST2* ORF was isolated from plasmid DAP106 and ligated into the corresponding sites of pUG34. Cells were grown to stationary phase in synthetic dextrose minimal medium (0.67% yeast nitrogen base without amino acids, 2% dextrose, 1.3 g of amino acid

dropout powder/600 ml) lacking histidine or both methionine and histidine on a rotary shaker at 30°C. Cells were diluted 1:100 in synthetic dextrose minimal medium lacking histidine or both methionine and histidine and grown to an optical density at 600 nm of 0.2. Vacuoles were stained with FM4-64 (Molecular Probes) and prepared for confocal microscopy as previously described (2). Confocal microscopy was performed with a Leica TCS SP microscope equipped with argon, krypton-argon, and UV lasers and 100 × 1.3NA lenses. Images were processed by using Photoshop 7.0 (Adobe).

Isolation of yeast vacuoles. Yeast cells grown to an optical density at 600 nm of 0.6 to 0.7 in 1 liter of medium were washed once with sterile distilled water and then once with 1.0 M sorbitol. Cells were converted to spheroplasts by suspension of the cell pellet in 100 ml of 1.0 M sorbitol containing 400 U of Zymolyase 100T (ICN Pharmaceuticals). The culture was gently shaken for 90 min at 30°C. Spheroplasts were collected by centrifugation at 800 × *g* for 5 min and then washed twice with 1.0 M sorbitol. All subsequent manipulations were carried out at 4°C. The pellet was suspended in 25 ml of buffer A (10 mM morpholineethanesulfonic acid [MES]-Tris [pH 6.9], 0.1 mM $MgCl_2$, 12% Ficoll 400) and homogenized by six or seven strokes in a Dounce homogenizer. The lysate was cleared by centrifugation at 26,600 × *g* for 35 min. The top wafer layer was collected and placed into a Dounce homogenizer containing 6 ml of buffer A, and clumps were broken up by six or seven strokes. The homogenate was transferred to an ultracentrifuge tube and layered with 6 ml of buffer B (10 mM MES-Tris [pH 6.9], 0.1 mM $MgCl_2$, 8% Ficoll 400). The mixture was centrifuged at 26,600 × *g* for 30 min. The top wafer layer was collected and placed into a tube containing 6 ml of buffer C (10 mM MES-Tris [pH 6.9], 5 mM $MgCl_2$, 25 mM KCl). Vacuoles were converted to vesicles by the addition of 2 volumes of buffer C, and a pellet was obtained by centrifugation at 26,600 × *g* for 20 min. The purity of the vacuoles obtained by this isolation procedure was verified by confocal microscopy, and vacuolar enrichment was confirmed by Western analysis with vacuolar markers (1, 12).

Assays of arginine transport. Arginine uptake assays were performed as previously described (13, 17, 18, 12). The accumulation of ^{14}C-arginine by vacuolar vesicles at each time point, at time zero, and at 30-s increments was assayed with a 100-μl reaction mixture composed of 25 mM Tris-MES (pH 7.4), 4 mM $MgCl_2$, 25 mM KCl, 0.3 mM ATP, 3.33 μCi of ^{14}C-arginine (348 mCi/mmol), and 30 μg of protein. The reaction was carried out at room temperature and was stopped by the addition of 5 ml of cold buffer C. Vacuolar vesicles were collected on a 0.22-μm-pore-size nylon membrane (Millipore, Burlington, Mass.). The radioactivity retained on the membrane was quantified with a scintillation counter (Beckman). The protein content of vacuolar preparations was assayed by using the Bradford assay (Bio-Rad).

RESULTS

Btn2p interacts with Ist2p. We used the Cytotrap two-hybrid system to screen for Btn2p interactions by cotransformation of yeast strain CDC25H with *BTN2*-pSOS and a yeast cDNA library in pMyr as previously described (2, 3). We had previously characterized Rhb1p and Yif1p as the most common candidates for interactions with Btn2p (2, 3). In addition, we isolated a single clone of *IST2* as a candidate for interactions (data not shown). As with all two-hybrid systems, biochemical or in vivo confirmation of interactions is required. Figure 1 shows Western analysis with an anti-c-*myc* monoclonal antibody and the same blot stripped and reprobed with an anti-FLAG monoclonal antibody for various yeast strains: a whole-cell extract from strain YPH499 that expresses only Btn2p tagged with FLAG at the C terminus (lane 1); a whole-cell extract from a strain expressing Btn2p-FLAG, which was immunoprecipitated with anti-FLAG monoclonal antibody (lane 2); a whole-cell extract from strain YPH499 that expresses both Ist2p tagged with c-*myc* and Btn2p tagged with FLAG and that shows the presence of Ist2p–c-*myc* (lane 3); and a whole-cell extract from a strain expressing both C-terminally c-*myc*-tagged Ist2p and C-terminally FLAG-tagged Btn2p, which was immunoprecipitated with anti-FLAG monoclonal antibody (lane 4). Immunoprecipitation with anti-FLAG antibody, which binds to FLAG-tagged Btn2p, brings with it c-*myc*-tagged Ist2p, confirming that Btn2p and Ist2p do physically interact in vivo. It should be noted that these tags do not alter the function of Btn2p (2) or Ist2p, as determined by the ability of the tagged proteins to complement the NaCl sensitivity of the growth of *btn2*Δ *ist2*Δ strains, a phenotype that is described later (see Fig. 3).

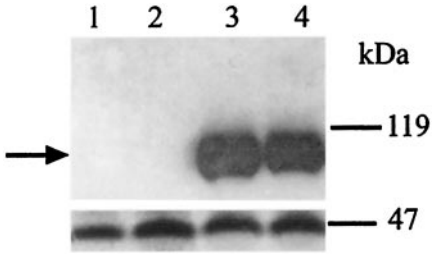

FIG. 1. Btn2p interacts with Ist2p in vivo. Immunoprecipitation was performed with anti-FLAG antibody and cell extracts derived from strain YPH499 expressing Btn2p-FLAG or both Btn2p-FLAG and Ist2p–c-*myc*. (Upper panel) Western analysis performed with anti-c-*myc* monoclonal antibody. (Lower panel) Western analysis performed with anti-FLAG monoclonal antibody. Lanes: 1, cell extract of YPH499 expressing Btn2p-FLAG; 2, cell extract of YPH499 expressing Btn2p-FLAG and immunoprecipitated with anti-FLAG antibody; 3, cell extract of YPH499 expressing Btn2p-FLAG and Ist2p–c-*myc*; 4, cell extract of YPH499 expressing Btn2p-FLAG and Ist2p–c-*myc* and immunoprecipitated with anti-FLAG antibody. Size markers are indicated on the right. The arrow indicates the Ist2p–c-*myc* band.

***btn2*Δ strains fail to localize Ist2p.** We previously reported that functional Btn2p-EGFP localized to the cytosol (2). Because the disruption of Btn2p function alters the localization of its interacting partners, Rhb1p and Yif1p, we tested whether the absence of Btn2p affected the localization of Ist2p. Ist2p has been reported to be localized at the plasma membrane (26). We confirmed that EGFP-Ist2p (N-terminal fusion of EGFP to Ist2p) in *ist2*Δ strains localizes to the plasma membrane (Fig. 2A). Furthermore, we demonstrated that in *btn2*Δ *ist2*Δ strains, EGFP-Ist2p is no longer localized to the plasma membrane but appears predominantly as a punctate entity in the cytosol (Fig. 2B). Interestingly, a small amount of EGFP-Ist2p appears to be localized in the vacuolar membrane; however, subcellular fractionation studies will be required to confirm this finding. These data suggest that the absence of Btn2p alters the localization of Ist2p and that Btn2p may therefore be involved in the trafficking or localization of Ist2p to the plasma membrane. Each image shown is typical of what was seen for the entire cell population for each strain. EGFP-Ist2p is functional, as determined by functional complementation of a phenotype that is described later (see Fig. 3). Note that Btn2p localization to the cytosol is not altered in *ist2*Δ strains (data not shown).

The growth of *btn2*Δ *ist2*Δ strains is NaCl sensitive. Ist2p has been reported to show similarity to higher eukaryotic sodium and calcium channel proteins (15). We therefore tested the sensitivity of the growth of *ist2*Δ strains to elevated concentrations of sodium or calcium in the media. Deletion of *IST2* was previously reported to result in salt tolerance (15); however, we found that *ist2*Δ strains did not show an obvious growth defect in the presence of elevated levels of sodium or calcium. However, *btn2*Δ *ist2*Δ strains failed to grow in media

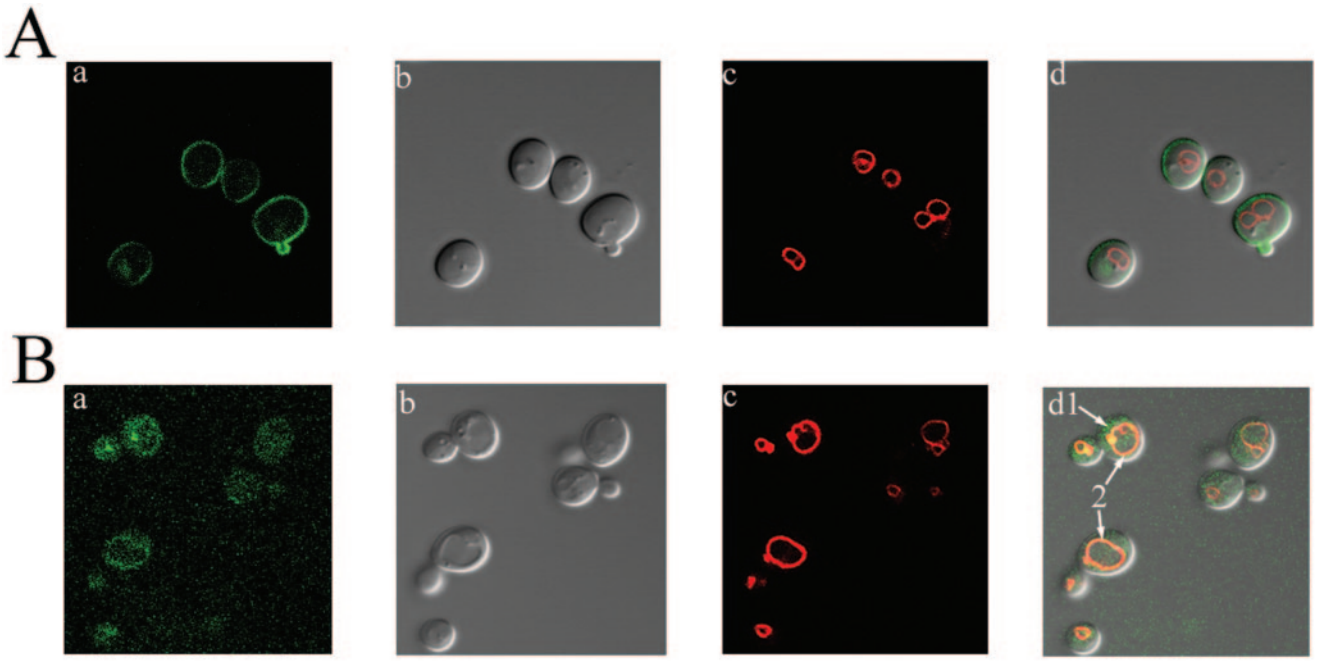

FIG. 2. Localization of Ist2p to the plasma membrane and alteration of the localization of Ist2p in *btn2*Δ strains. (A) EGFP-Ist2p in *ist2*Δ strain B-14915. (B) EGFP-Ist2p in *btn2*Δ *ist2*Δ strain B-14983. (a) EGFP fluorescence. (b) Differential interference contrast images. (c) FM4-64 staining showing the vacuolar membrane. (d) Merged images. EGFP-Ist2p in the *ist2*Δ strain localizes to the plasma membrane. EGFP-Ist2p in the *btn2*Δ *ist2*Δ strain appears to be mislocalized to the cytoplasm and the vacuolar membrane (arrows 1 and 2, respectively). Each image is presented at a magnification of ×100 and is typical of that seen for the entire cell population.

containing 0.5 or 1.0 M NaCl (Fig. 3). There was no effect on growth for the same strains in the presence of elevated calcium levels (data not shown). We also found that deletion of Rhb1p, which also interacts with Btn2p, does not result in an NaCl sensitivity phenotype. Furthermore, deletion of Ist2p does not result in the canavanine resistance phenotype previously reported for strains lacking Rhb1p or Btn2p (2). The NaCl sensitivity phenotype exhibited by *btn2*Δ *ist2*Δ strains could be complemented by the expression of plasmid-borne *BTN2* or *IST2* (data not shown) and by c-*myc*- or EGFP-tagged *IST2*, as shown in the coimmunoprecipitation and localization studies described above, respectively (Fig. 3).

The growth of *btn1*Δ *ist2*Δ strains is also NaCl sensitive. Btn2p was originally identified as being up-regulated in a *btn1*Δ strain. We therefore tested whether *btn1*Δ results in sensitivity of growth in media containing NaCl. Although the growth of *btn1*Δ strains did not show NaCl sensitivity, *btn1*Δ *btn2*Δ and *btn1*Δ *ist2*Δ strains were both unable to grow in

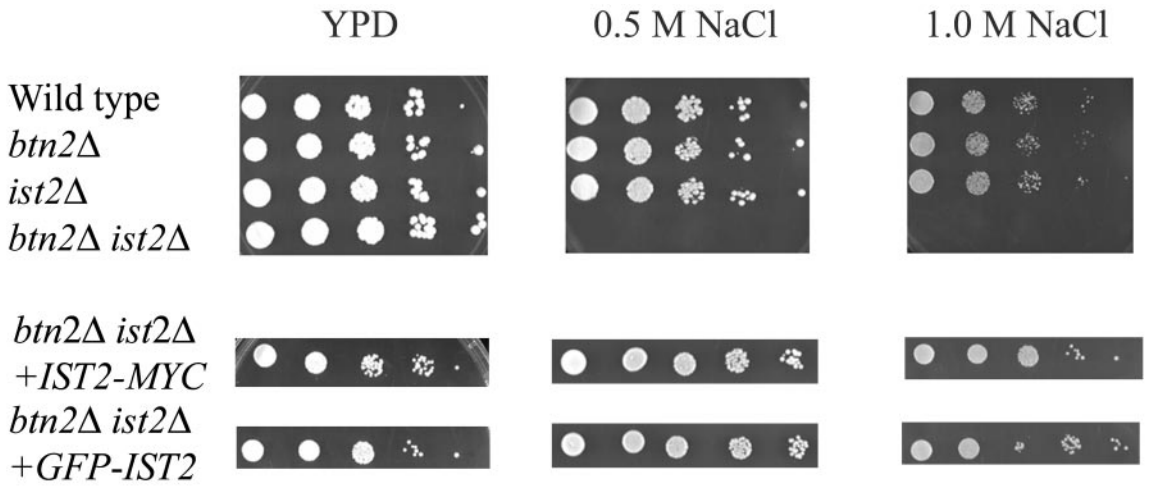

FIG. 3. *btn2*Δ *ist2*Δ strains are sensitive to NaCl. Wild-type (B-11718), *ist2*Δ (B-14884), *btn2*Δ (B-14847), and *btn2*Δ *ist2*Δ (B-15013) strains were serially diluted. Wild-type, *ist2*Δ, and *btn2*Δ cells grew normally, whereas *btn2*Δ *ist2*Δ cells exhibited sensitivity of growth. Plates were incubated at 30°C for 2 days. For complementation studies, *IST2*–c-*myc* and EGFP-*IST2* were independently subcloned into centromeric single-copy expression vector pAB625 and similarly plated (1).

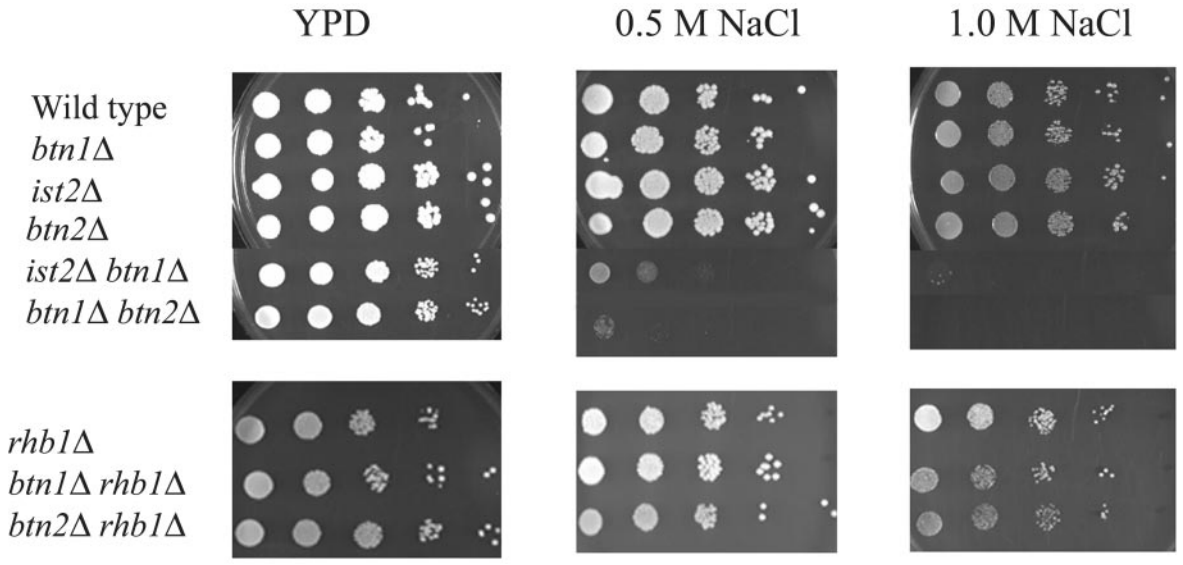

FIG. 4. *btn1*Δ *ist2*Δ strains are sensitive to NaCl. Wild-type (B-11718), *ist2*Δ (B-14884), *btn1*Δ (B-13048), *btn2*Δ (B-14847), *btn1*Δ *ist2*Δ (B-14830), and *btn1*Δ *btn2*Δ (B-13049) strains were serially diluted. Wild type, *ist2*Δ, *btn2*Δ, and *btn1*Δ cells grew normally, whereas *ist2*Δ *btn1*Δ and *btn1*Δ *btn2*Δ strains exhibited sensitivity of growth. Note that strains with a deletion of *RHB1* (*rhb1*Δ, *btn1*Δ *rhb1*Δ, and *btn2*Δ *rhb1*Δ strains) did not show a similar genetic interaction. Plates were incubated at 30°C for 2 days.

media containing 0.5 or 1.0 M NaCl (Fig. 4). Because Btn2p has been shown to interact with Rhb1p, we demonstrated that the growth of *btn1*Δ *rhb1*Δ and *btn2*Δ *rhb1*Δ strains did not show NaCl sensitivity. Therefore, the NaCl sensitivity phenotype is not a result of interactions with Btn2p but is a result of the loss of distinct interactions between Btn2p and Ist2p or Btn1p and Ist2p. Strains lacking Yif1p, which also interacts with Btn2p, could not be tested, as this is an essential protein.

We also performed FM4-64 staining to test the vacuolar integrity and morphology of cells exposed to NaCl. We found that strains containing *btn1*Δ appear to have more fragmented vacuoles. However, as the dynamics of this technique have not been fully characterized in the presence of high salt concentrations, we report this finding as a qualitative assessment while we work to establish a reliable means of isolating vacuoles from salt-exposed strains to quantify the possible effects that NaCl may have on vacuoles of *btn1*Δ strains as opposed to other strains.

***ist2*Δ suppresses the defect in vacuolar arginine transport in *btn1*Δ strains.** We previously reported that vacuoles isolated from *btn1*Δ strains have a decreased ability to transport arginine into the lumen of this organelle (12). To test whether

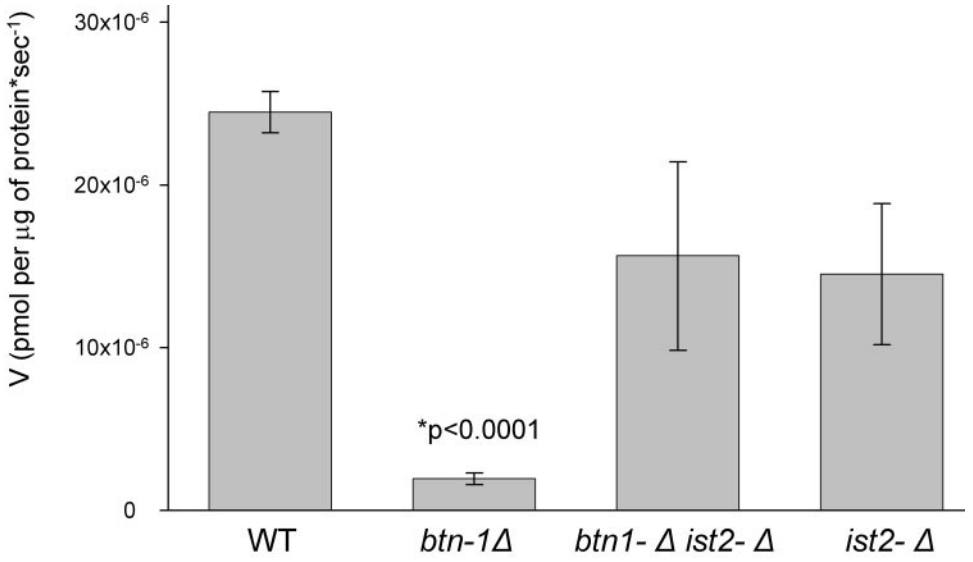

FIG. 5. *ist2*Δ suppresses the decrease in the rate of vacuolar arginine uptake in isolated vacuoles caused by *btn1*Δ. The rates of uptake of ^{14}C-arginine into isolated vacuoles from wild-type (WT) (B-11718), *btn1*Δ (B-13048), *ist2*Δ (B-14884), and *btn1*Δ *ist2*Δ (B-14830) strains are shown. Note that all isolated vacuoles were prepared from strains grown on YPD medium.

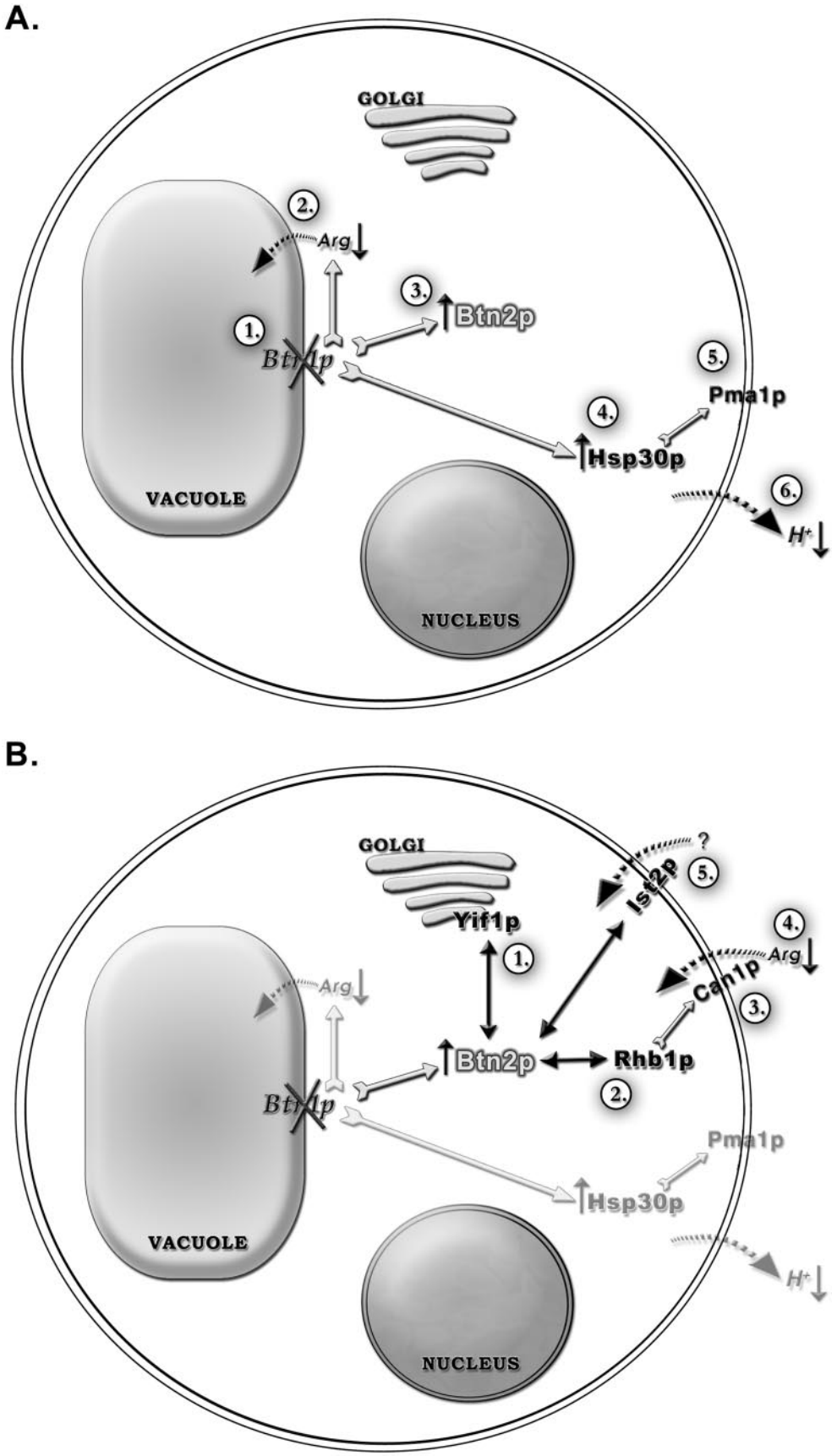
A.
GOLGI
2.
Arg
3.
Btn2p
1.
Btr1p
5.
Pma1p
4.
Hsp30p
6.
H+
VACUOLE
NUCLEUS
B.
GOLGI
?
Ist2p
5.
Yif1p
1.
4.
Arg
Can1p
3.
Arg
Btn2p
Rhb1p
2.
Btr1p
Pma1p
Hsp30p
H+
VACUOLE
NUCLEUS

Ist2p exerts an effect on the transport of arginine into the vacuole, we examined the effect of deleting *IST2* (*ist2*Δ) on vacuolar arginine transport. Compared to the wild type, *ist2*Δ did not significantly alter arginine transport into the vacuole (Fig. 5). However, *btn1*Δ *ist2*Δ strains showed nearly normal levels of arginine transport into the vacuole, indicating that *ist2*Δ suppressed this defect in *btn1*Δ strains and revealing a distinct interaction between Btn1p and Ist2p.

DISCUSSION

BTN2 encodes a 410-amino-acid novel coiled-coil protein that has a role in localizing proteins to different subcellular compartments. Btn2p was originally identified as being up-regulated in a *btn1*Δ strain. The functional implications of Btn1p and Btn2p interactions as a result of *btn1*Δ are summarized in Fig. 6. Btn1p is a vacuolar protein, and *btn1*Δ results in altered vacuolar pH and decreased sequestration of the basic amino acids arginine and lysine in the vacuole (Fig. 6A) (4, 12, 24). A previous study revealed that *btn2*Δ results in elevated activity of the vacuolar H^+-ATPase, suggesting that the up-regulation of *BTN2* expression in *btn1*Δ strains may contribute either directly or indirectly to normalization of the vacuolar pH in *btn1*Δ strains (24). However, *btn2*Δ does not result in altered vacuolar pH, and *btn1*Δ does not result in altered vacuolar H^+-ATPase activity, suggesting that there is no direct correlation between vacuolar pH and vacuolar H^+-ATPase activity (1). Interestingly, the only other gene up-regulated in *btn1*Δ strains in addition to *BTN2* is *HSP30* (24). The up-regulation of *HSP30* was shown to down-regulate the activity of the plasma membrane H^+-ATPase, which was presumed to result in elevated use of ATP as well as elevated proton pumping out of the cell (Fig. 6A). However, as we discuss below, we now believe that *btn1*Δ results in an alteration in ion homeostasis, perhaps due to altered amino acid levels, and this alteration in the regulation of plasma membrane H^+-ATPase activity through Hsp30p could be interpreted as a means of balancing the ionic content of cells.

Btn2p is a cytosolic protein that has now been implicated in localizing Rhb1p to the cell periphery, Yif1p to the Golgi apparatus, and now Ist2p to the plasma membrane (Fig. 6B). There is little to link Rhb1p, Yif1p, and Ist2p at the functional level other than the fact that each interacts with Btn2p and that each is mislocalized in the absence of Btn2p. We have therefore discovered a novel link among Rhb1p, Yif1p, and Ist2p that implies that Btn2p has the potential to affect several cellular processes. Disruption of Btn2p function can result in a variety of different phenotypes that are associated with the mislocalization of Btn2p-interacting proteins. In this study, we have shown that Btn2p physically interacts with Ist2p and that Btn2p is necessary for the correct localization of Ist2p. In addition, we have shown that *btn2*Δ or *btn1*Δ in combination with *ist2*Δ results in a similar phenotype, sensitivity to NaCl. The role of Btn2p and its multiple interactions are summarized in Fig. 6B. Btn2p may have a role in regulating the trafficking around the cell of a very specific set of proteins that have a functional link essential to maintaining a biological balance. In this sense, Btn2p may be a sensor of an imbalance or an effector that acts upon an imbalance. What Btn2p senses or responds to requires further study. However, clues that further identify the role of Btn2p come from studies of *btn1*Δ strains that up-regulate Btn2p, which are further discussed below and which suggest that Btn2p may have a role in sensing or responding to changes in cation levels in cells.

We demonstrate that *btn1*Δ strains lacking either Ist2p or Btn2p show decreased growth in the presence of high salt concentrations. Several Na^+/H^+ antiporters present in the vacuolar membrane have been implicated as functioning in vacuolar transport, vacuolar acidification, and ion homeostasis (10). Furthermore, several studies have concluded that H^+ antiporters represent the principal mechanism of transporting both inorganic and organic cations across the vacuolar membrane (19). In addition, a family of seven proteins has been identified as mediating bidirectional amino acid transport at the vacuolar membrane (25). Btn1p has been shown to be involved in the transport of arginine into the vacuole (12), and arginine transport across the vacuolar membrane requires the generation of a proton motive force and an intact vacuolar ATPase (12, 17, 25). Disruption of Btn1p function disrupts the transport of arginine into the vacuole, resulting in a 10-fold decrease in the levels of sequestered arginine and lysine in the vacuole (12). Therefore, one could predict that an environmental insult, such as high salt concentrations, would alter the activity of vacuolar Na^+/H^+ antiporters and precipitate further disruptions in transport processes at the vacuolar membrane. Thus, disruption of both Btn1p at the vacuole and Ist2p at the plasma membrane (*btn1*Δ *ist2*Δ strains) results in cells being unable to maintain cellular cationic balance upon exposure to high salt concentrations. Similarly, the lack of Btn2p and its multiple roles in cells precipitate a similar situation in *btn1*Δ *btn2*Δ and *btn1*Δ *ist2*Δ strains.

It is fascinating that *ist2*Δ suppresses the vacuolar arginine transport defect exhibited by *btn1*Δ strains. Although further studies are required, it is apparent that disruptions that result in altered cation levels, whether they are organic, such as arginine, or inorganic, such as salt, have revealed a link that indicates that yeast cells may work to maintain an overall ionic balance of all or some of these ions. Although there appears to be no apparent correlation between vacuolar pH and vacuolar

FIG. 6. Schematic representation of the cellular roles of Btn1p and Btn2p. (A) Step 1 shows the deletion of *btn1*Δ. Step 2 shows that *btn1*Δ results in decreased arginine uptake into the vacuole (12). Step 3 shows that *btn1*Δ results in the up-regulation of Btn2p (23). Step 4 shows that *btn1*Δ results in the up-regulation of Hsp30p (11, 23). Step 5 shows that the up-regulation of Hsp30p down-regulates overactive Pma1p (23). Step 6 shows that the up-regulation of Hsp30p decreases excess proton pumping across the plasma membrane (23). (B) Step 1 shows that Btn2p interacts with Yif1p and is involved in correctly localizing this protein to the Golgi apparatus (3). Step 2 shows that Btn2p interacts with and is involved in correctly localizating Rhb1p (2). Step 3 shows that Rhb1p negatively regulates the Can1p permease, which transports arginine and lysine into the cell (27). Step 4 shows decreased uptake of arginine into the cell (2). Step 5 shows that Btn2p interacts with Ist2p, which shows homology to ion channel proteins and may be involved in the transport of an as-yet-unidentified cation across the plasma membrane.

H^+-ATPase activity, future experiments will focus on determining whether cation levels influence both vacuolar pH and vacuolar H^+-ATPase activity. We note that studies of other organisms have revealed that plants have been shown to mediate salt tolerance through ion uptake into the tonoplast (28). A complete understanding of this phenomenon, in particular, in *btn1*Δ strains, will require a complete understanding of which proteins facilitate the transport of all molecules into and out of cells and also into and out of each subcellular compartment.

It was previously demonstrated that the protein associated with Batten disease, Cln3, and Btn1p have conserved functions. Btn1p is 39% identical and 59% similar to human Cln3 protein, mutations in which result in the lysosomal storage disorder Batten disease (11, 22). Batten disease is characterized by accumulation of lipopigments in the lysosome (6, 8, 14, 20, 21). In summary, *btn1*Δ cells are known to have an altered regulation of vacuolar pH and a decrease in the ability to transport basic amino acids into the vacuole, features which presumably account for the decreased levels of basic amino acids in the vacuole. Our new findings suggest that these alterations in vacuolar content might result in these cells having an altered ability to maintain cellular and vacuolar ionic homeostasis. A limited ability to utilize the vacuolar compartment as a means to maintain ionic homeostasis might precipitate further vacuolar-lysosomal dysfunction. It is obviously difficult to compare ion homeostasis mechanisms between single-celled organisms, such as yeasts, and humans. However, a change in lysosomal function mediated by altered ionic content could conceivably result in the accumulation or aggregation of proteins that are usually targeted to the lysosome for degradation and might contribute to the characteristic accumulation of storage materials in the lysosome in Batten disease.

ACKNOWLEDGMENTS

We thank Tim Curran for technical support and Denia Ramirez-Montealegre and Jared Benedict for help in preparation of the manuscript.

This work was supported by NIH grant R01 NS36610. S.J.L. was supported by grant NSF9986712 from the REU Program in Cellular and Molecular Biology at the University of Rochester.

REFERENCES

1. **Chattopadhyay, S., N. E. Muzaffar, F. Sherman, and D. A. Pearce.** 2000. The yeast model for Batten disease: mutations in BTN1, BTN2, and HSP30 alter pH homeostasis. J. Bacteriol. **182:**6418–6423.
2. **Chattopadhyay, S., and D. A. Pearce.** 2002. Interaction with Btn2p is required for localization of Rsg1p: Btn2p-mediated changes in arginine uptake in *Saccharomyces cerevisiae*. Eukaryot. Cell **1:**606–612.
3. **Chattopadhyay, S., P. M. Roberts, and D. A. Pearce.** 2003. The yeast model for Batten disease: a role for Btn2p in the trafficking of the Golgi-associated vesicular targeting protein, Yif1p. Biochem. Biophys. Res. Commun. **302:** 534–538.
4. **Croopnick, J. B., H. C. Choi, and D. M. Mueller.** 1998. The subcellular location of the yeast *Saccharomyces cerevisiae* homologue of the protein defective in the juvenile form of Batten disease. Biochem. Biophys. Res. Commun. **250:**335–341.
5. **Entian, K. D., et al.** 1999. Functional analysis of 150 deletion mutants in Saccharomyces cerevisiae by a systematic approach. Mol. Gen. Genet. **262:** 683–702.
6. **Goebel, H. H.** 1995. The neuronal ceroid lipofuscinoses. J. Child Neurol. **10:**424–437.
7. **Guldener, U., S. Heck, T. Fielder, J. Beinhauer, and J. H. Hegemann.**1996. A new efficient gene disruption cassette for repeated use in budding yeast. Nucleic Acids Res. **24:**2519–2524.
8. **Hall, N. A., B. D. Lake, N. N. Dewji, and N. D. Patrick.** 1991. Lysosomal storage of subunit *c* of mitochondrial ATP synthase in Batten's disease. Biochem. J. **275:**269–272.
9. **Haskell, R. E., C. J. Carr, D. A. Pearce, M. J. Bennett, and B. L. Davidson.** 2000. Batten disease: evaluation of CLN3 mutations on protein localization and function. Hum. Mol. Genet. **9:**735–744.
10. **Hirata, T., Y. Wada, and M. Futai.** 2002. Sodium and sulfate ion transport in yeast vacuoles. J. Biochem. **131:**261–265.
11. **International Batten Disease Consortium.** 1995. Isolation of a novel gene underlying Batten disease. Cell **82:**949–957.
12. **Kim, Y., D. Ramirez-Montealegre, and D. A. Pearce.** 2003. A role in vacuolar arginine transport for yeast Btn1p and human CLN3, the protein defective in Batten disease. Proc. Natl. Acad. Sci. USA **100:**15458–15462.
13. **Kitamoto, K., K. Yoshizawa, Y. Ohsumi, and Y. Anraku.** 1988. Mutants of *Saccharomyces cerevisiae* with defective vacuolar function. J. Bacteriol. **170:** 2687–2691.
14. **Kominami, E., J. Ezaki, D. Muno, K. Ishido, T. Ueno, and L. S. Wolfe.** 1992. Specific storage of subunit c of mitochondrial ATP synthase in lysosomes of neuronal ceroid lipofuscinosis (Batten's disease) J. Biochem. **111:**278–282.
15. **Mannhaupt, G., R. Stucka, S. Ehnle, I. Vetter, and H. Feldmann.** 1994. Analysis of a 70Kb region on the right arm of yeast chromosome II. Yeast **10:**1363–1381.
16. **Matern, H., X. Yang, E. Andrulis, R. Sternglanz, H.-H. Trepte, and D. Gallwitz.** 2000. A novel Golgi membrane protein is part of a GTPase-binding protein complex involved in vesicle targeting. EMBO J. **19:**4485–4492.
17. **Ohsumi, Y., and Y. Anraku.** 1981. Active transport of basic amino acids driven by a proton motive force in vacuolar membrane vesicles of Saccharomyces cerevisiae. J. Biol. Chem. **256:**2079–2082.
18. **Ohsumi, Y., K. Kitamoto, and Y. Anraku.** 1988. Changes induced in the permeability barrier of the yeast plasma membrane by cupric ion. J. Bacteriol. **170:**2676–2682.
19. **Okorokov, L. A., T. V. Kulakovskaya, L. P. Lichto, and L. V. Polorotova.** 1985. H^+/ion antiport as the principal mechanism of transport systems in the vacuolar membrane of the yeast Saccharomyces carlsbergensis. FEBS Lett. **192:**303–306.
20. **Palmer, D. N., I. M. Fearnley, J. E. Walker, N. A. Hall, B. D. Lake, L. S. Wolfe, M. Haltia, R. D. Martinur, and R. D. Jolly.** 1992. Mitochondrial ATP synthase subunit *c* storage in the ceroid-lipofuscinoses (Batten disease). Am. J. Med. Genet. **42:**561–567.
21. **Palmer, D. N., S. L. Bayliss, and V. J. Westlake.** 1995. Batten disease and the ATP synthase subunit *c* turnover pathway: raising antibodies to subunit *c*. Am. J. Med. Genet. **57:**260–265.
22. **Pearce, D. A., and F. Sherman.** 1997. BTN1, a yeast gene corresponding to the human gene responsible for Batten's disease, is not essential for viability, mitochondrial function, or degradation of mitochondrial ATP synthase. Yeast **13:**691–697.
23. **Pearce, D. A., and F. Sherman.** 1998. A yeast model for the study of Batten disease. Proc. Natl. Acad. Sci. USA **95:**6915–6918.
24. **Pearce, D. A., T. Ferea, S. A. Nosel, B. Das, and F. Sherman.** 1999. Action of Btn1p, the yeast orthologue of the gene mutated in Batten disease. Nat. Genet. **22:**55–58.
25. **Russnak, R., D. Konczal, and S. L. McIntire.** 2001. A family of yeast proteins mediating bidirectional vacuolar amino acid transport. J. Biol. Chem. **276:** 23849–23857.
26. **Takizawa, P. A., J. L. DeRisi, J. E. Wilhelm, and R. D. Vale.** 2000. Plasma membrane compartmentalization in yeast by messenger RNA transport and a septin diffusion barrier. Science **290:**341–344.
27. **Urano, J., A. P. Tabancay, W. Yang, and F. Tamanoi.** 2000. The *Saccharomyces cerevisiae* Rheb G-protein is involved in regulating canavanine resistance and arginine uptake. J. Biol Chem. **275:**11198–11206.
28. **Wang, B., U. Luttge, and R. Ratajczak.** 2001. Effects of salt treatment and osmotic stress on V-ATPase and V-PPase in leaves of the halophyte Suaeda salsa. J. Exp. Bot. **52:**2355–2365.